Structure within Thin Epoxy Films Revealed by Solvent Swelling: A Neutron Reflectivity Study

H. Yim, M. Kent,* and W. F. McNamara

Department 1832, Sandia National Laboratories, Albuquerque, New Mexico

R. Ivkov and S. Satija

National Institute of Standards and Technology, Gaithersburg, Maryland

J. Majewski

LANCSE, Los Alamos National Laboratories, Los Alamos, New Mexico

Received June 22, 1999

ABSTRACT: Structure within thin epoxy films is investigated by neutron reflectivity (NR) as a function of resin/cross-linker composition and cure temperature. Variation in the cross-link density normal to the substrate surface is examined by swelling the films with the good solvent *d*-nitrobenzene (d-NB). The principal observation is a large excess of d-NB near the air surface. *This is not a wetting layer*, but rather indicates a lower cross-link density in the near-surface region. This effect is due to preferential segregation of the cross-linker to the air surface, driven by the lower surface tension of the cross-linker relative to the epoxide oligomers. The magnitude of the effect is a function of composition and cure temperature. Exclusion of d-NB from the region immediately adjacent to the substrate surface is also observed, possibly indicating a tightly bound layer of epoxy. Regarding swelling in the bulk of the films, the behavior is nonsymmetric with departure from the stoichiometric ratio. The films deficient in curing agent show greater equilibrium swelling and faster swelling kinetics than the films with an excess of curing agent.
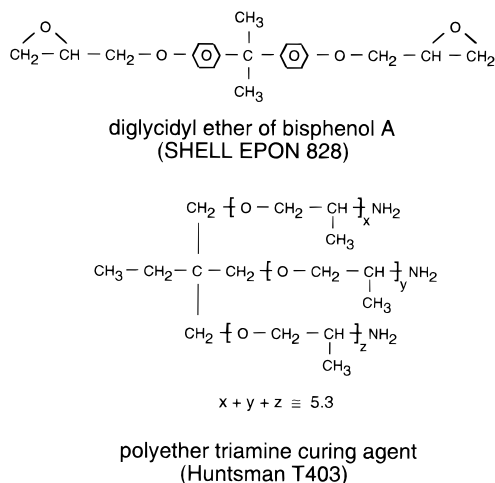
Introduction

Due to a variety of factors, the structure and properties of polymer films can be different near interfaces compared to the bulk. At a substrate surface, polymer mobility is generally restricted due to adsorption of segments, restricted conformations, segment layering, alignment of chains, and decreased free volume.[1−5] Diffusion of small molecule probes appears to be less affected, with some studies showing a slightly reduced mobility within a polymer film near a substrate surface and others showing little or no reduction in mobility.[6−8] At the air surface of glassy polymers, mobility is typically increased relative to the bulk.[9−13] In multi-component systems, preferential segregation can occur at either interface due to both enthalpic and entropic effects.[14−17] Similar considerations also drive segregation of chain ends to interfaces.[18−26] Kinetic effects have been shown to be important in the resulting structure of spin-cast films of glassy polymers.[27−29]

Structure near a substrate surface is important for stress transfer, mechanical properties, fracture mechanisms, and diffusion of penetrants, among others. Structure at the air surface can impact surface reconstruction, surface free energy, wettability, and reactivity. In addition, structural gradients at air interfaces can impact the interfacial strength that develops when contacted with a second polymer. This is particularly important in technological applications involving multiple thermosets such as multilayer paint films and manufacturing processes involving multiple adhesives and encapsulants that come into contact.

Our focus is the structure within highly cross-linked, two-component epoxy films. In such systems, preferential segregation of either component to an interface will strongly effect the structure by altering the local stoichiometry and, therefore, the cross-link density. Variation in stoichiometry can affect not just the average cross-link density but also the distribution of cycles and dangling ends.[30] Several workers have reported evidence of gradients in cross-link density at substrate surfaces in such systems,[31−39] in some cases extending to ~1000 Å from the substrate surface.[31−33,36] In addition to segregation at interfaces, unreacted monomer can segregate from high molecular weight gel fractions during cure, leading to heterogeneity within the bulk of the film.[39] In such systems, the rate of the cross-linking reaction(s) and the rate of segregation can be in competition. With a rapidly cured system, segregation will be minimized, whereas equilibrium interfacial concentration profiles and segregation within the bulk are expected for very slowly curing systems. Thus, cure rate is an important aspect explored in this work.

We examine variations in cross-link density within thin (600−1200 Å) epoxy films on silicon substrates by solvent swelling. The method is based on the fact that the equilibrium volume fraction of a swelling solvent is strongly dependent upon the local cross-link density. We examine the volume fraction profile of the good solvent nitrobenzene through the epoxy films by neutron reflection. Isotopic substitution is used to provide contrast between the epoxy matrix and the swelling solvent. Swelling is an important method that has been employed for many years to determine the average cross-link density in macroscopic bulk samples.[40] Variation in local swelling has been used to examine the degree of structural heterogeneity within the bulk of cross-linked samples by neutron scattering.[41−45] Wu et al. examined the swelling of a bulk epoxy sample cross-linked with a linear diamine.[44] Their data are consistent with a heterogeneous distribution of cross-links. However, the absence of any peaks in the scattering data

diglycidyl ether of bisphenol A
(SHELL EPON 828)

$x + y + z \cong 5.3$

polyether triamine curing agent
(Huntsman T403)

Figure 1. Chemical structure of DGEBA epoxy resin and T403 polyethertriamine curing agent.

indicates the absence of a well-defined correlation length in the heterogeneous network structure. In particular, their data are not consistent with the presence of well-defined nodules as have been reported in some systems.[39]

Following a description of the experimental details, the results are presented in two sections. The first deals with the equilibrium swelling as a function of stoichiometry and cure temperature. In the second section we examine the swelling as a function of time prior to attaining equilibrium.

Experimental Section

Materials. Research grade EPON 828 epoxy resin was obtained from Shell Chemical Co.[46] The resin was cured with an aliphatic polyethertriamine (T403, Huntsman Chemical). Both resin and cross-linker were used as received. The chemical structures of the amine and epoxide monomers are shown in Figure 1. If these monomers combine exclusively through epoxide–amine addition reactions, about 46 amine parts per 100 epoxide parts by weight (phr = parts per hundred resin) are required for complete cure. This is consistent with experimental measurements of the maximum glass transition temperature and the minimum swelling ratio.[30] To prepare uniform thin films by spin-coating onto silicon wafers, it was necessary to increase the molecular weight prior to spin-coating. This was accomplished by heating the resin and cross-linker mixtures at 60 °C for 70 min. The mixtures were then dissolved in toluene for spin-coating. Three solutions with different concentrations of T403 (36, 46, and 56 phr) were prepared. An aliquot of each solution was deposited onto a silicon wafer using a glass pipet and then spun off at 3000 rpm using a Headway photoresist spinner. The silicon wafers used as substrates in this study were polished 2 in. diameter single crystals (111) obtained from Semiconductor Processing Co. The wafers were cleaned using the "RCA" process: a sulfuric acid/hydrogen peroxide clean, followed by etching in an HF solution, and then the regrowth of silicon oxide with ammonium hydroxide/hydrogen peroxide solution. Two films were prepared for each mixture to examine the effect of curing temperature. One set of three samples (36, 46, and 56 phr) was cured at 50 °C for 48 h (cure A), while the second set of samples was cured at 80 °C for 1 h and then 120 °C for 2 h (cure B). Our goal was to achieve full cure with each condition. A previous study of this system indicates that full cure is achieved at 50 °C in roughly 24 h for the 36 phr composition.[47] However, no data are currently available for the 46 and 56 phr compositions, and we now suspect that the 46 phr films may not be fully cured with cure A. We will return to this point later in the Results and Discussion section. Following cure,

Table 1. Calculated Neutron Scattering Length Densities (b/V, 10^{-4} Å^{-2}) of the Materials Used in This Study[a]

	b/V		b/V
d-NB	0.0555	46 phr mixture	0.0113
EPON 828	0.0151	56 phr mixture	0.0107
T403	0.0029	silicon	0.0207
36 phr mixture	0.0119	silicon oxide	0.0300

[a] The following densities were used in the calculations: $\rho_{T403} = 0.98$, $\rho_{EPON\ 828} = 1.17$.

the samples were desiccated until the reflectivity measurements were performed.

Methods. The surface tensions of the liquid epoxy resin, cross-linker, and resin/cross-linker mixtures were measured by the Wilhelmy plate technique using a sandblasted platinum plate and a Q11 force transducer from Hottinger Baldwin Measurements.

Neutron reflectivity (NR) measurements were performed on the NG7 reflectometer (NIST). A fixed wavelength of 4.74 Å was used. The intensity of reflected neutrons is measured as a function of momentum transfer ($q = 4\pi \sin \theta/\lambda$, where θ is the angle of incidence and λ is the wavelength). Such reflectivity curves are very sensitive to the 1-dimensional profile of the neutron scattering length density (SLD) normal to the substrate surface. The neutron SLD is a function of the density and atomic composition. The calculated SLD values of the materials used in this work are shown in Table 1. During the measurements, the samples were maintained at room temperature in a sealed aluminum chamber. The reflectivity of the as-prepared samples was first measured with desiccant in the chamber. The desiccant was then removed, and the chamber was saturated with *d*-nitrobenzene (d-NB), a good solvent for both the resin and the cross-linker. Since the surface tension of d-NB ($\sim$48 mN/m) is higher than that of the mixtures of epoxy resin and T403 ($\sim$34–37 mN/m), a wetting layer of d-NB does not form on the surface of the epoxy film. This was important since the neutron beam was directed onto the interface from the air side. Equilibrium saturation of d-NB within the films was confirmed by measuring the reflectivity with time until no further change was observed.

The SLD profiles cannot be obtained by direct inversion of the reflectivity data, but rather are obtained from a fitting procedure. This involves approximating the model profiles by a series of slabs of constant concentration and then calculating the reflectivity from the stack of layers using the optical matrix method.[48] The effects of roughness and finite interface width are included by dividing each interface into a number of small slabs to form a smooth gradient. Both the interface width and the functional form of the gradient can be varied. The resolution, $\Delta q/q$ where Δq is the standard deviation of a Gaussian function, was fixed at 0.02. Best-fit parameters were determined by the minimization of χ^2 using the Marquardt algorithm.
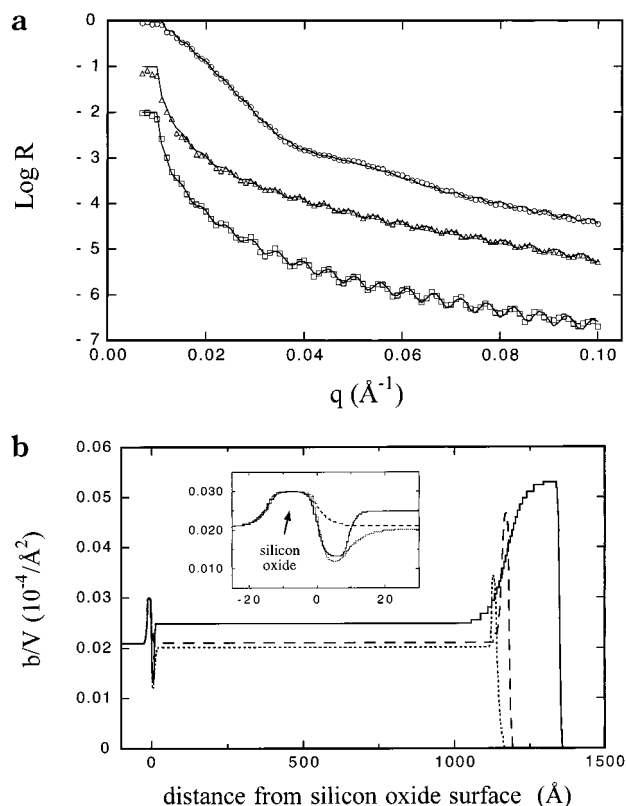
Results and Discussion

Equilibrated Films. Reflectivity from a 46 phr sample (cure A) as-prepared and after swelling to equilibrium with d-NB is shown in Figure 2a. With the low-temperature cure, we expect that equilibrium composition profiles at the interfaces are approached prior to cross-linking. The reflectivity for the as-prepared sample shows strong oscillations that persist to the highest values of q examined. This indicates that the epoxy film is quite smooth. The curve through the data for the as-prepared sample corresponds to the best fit using a single layer profile for the epoxy film shown by the solid line in Figure 2b. The SLD is consistent with that calculated from the atomic composition and the density given in Table 1. The roughness at the air surface corresponds to $\sigma = 4$ Å, where σ is defined as the root-mean-square (rms) value of the deviation of the
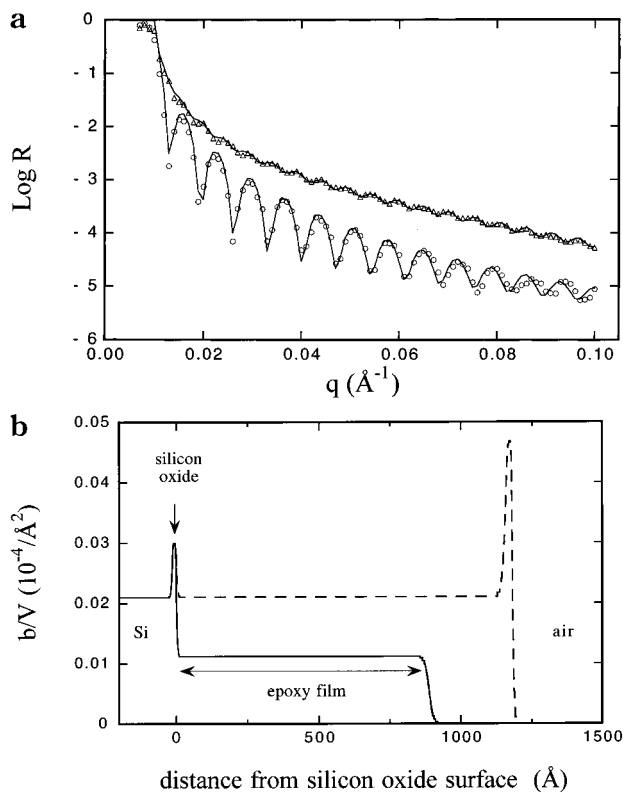
Figure 2. (a) Neutron reflectivity data from a 46 phr sample (cure A) as-prepared (O) and after swelling to equilibrium with d-NB (△). The curves through the data correspond to best fits using model scattering length density profiles. (b) Best-fit scattering length density profiles corresponding to the curves through the data in (a) for the sample as-prepared (—) and after swelling (- - -).

Figure 3. (a) Neutron reflectivity data from 36 (O), 46 (△), and 56 phr (□) samples (cure A) after swelling to equilibrium with d-NB. The data have been shifted on the *y*-axis for clarity. The curves through the data correspond to best fits using model scattering length density profiles. (b) Best-fit scattering length density profiles corresponding to the curves through the data in (a) for 36 (—), 46 (- - -), and 56 phr (· · ·) samples. The inset shows the depletion layer of d-NB at the substrate surface.

height relative to the average height of the surface. This simple model is entirely adequate to describe the data for the as-prepared sample. Similar profiles were also adequate for the as-prepared 36 and 56 phr samples. In each case, the reflectivity data could be described using a single-step profile with roughness at the air surface comparable to that for the 46 phr sample.

In Figure 2a, the 46 phr sample swollen with d-NB shows a large increase in reflectivity relative to the data for the as-prepared sample. The increase is due to adsorption of d-NB. The best-fit SLD profile for the d-NB swollen sample is also shown in Figure 2b. The thickness and SLD of the swelled film have both increased substantially relative to that of the as-prepared film. More importantly, in contrast with the results for the as-prepared sample, the reflectivity for the swelled sample is not consistent with a single layer profile, but rather increased SLD is required at the air surface. This indicates excess d-NB and thus a lower cross-link density in the region near the air surface. This effect is due to preferential segregation of the polyetheramine cross-linker to the air surface. Segregation of T403 to the air surface is expected on the basis of the surface tensions of the resin (47.8 mN/m) and the cross-linker (33.5 mN/m). The surface tensions for the 36, 46, and 56 phr mixtures were measured to be 36.7, 35.2, and 34.0 mN/m, respectively. The fact that the surface tensions of the mixtures are close to the value for pure T403 verifies that the surface is rich in T403. Segregation of low surface energy components to the air surface has been studied extensively in other multicomponent polymer films.[14-17]

Figure 3a compares NR data from 36, 46, and 56 phr films with cure A after swelling to equilibrium with d-NB. The SLD profiles are shown in Figure 3b. Note that the form of the reflectivity curve is different for each film. These data reveal several important differences in the structure of the epoxy films. For the 36 phr film the reflectivity curve shows very high reflectivity at low q (0.01 Å^{-1} < q < 0.04 Å^{-1}). Without any detailed analysis, the enhanced reflectivity at low q for the 36 phr film is a clear indication of much greater absorption of d-NB near the air surface. The magnitude of this effect for the three compositions occurs in the following order: 36 phr ≫ 46 phr > 56 phr. This trend can be understood by considering the composition perturbation near the air surface to consist of two layers as illustrated in Figure 4: an excess of T403 immediately at the surface followed by a layer that we will refer to as the "near-surface" layer which is depleted of T403. A 36 phr film would be deficient in T403 if resin and cross-linker were uniformly distributed. Strong segregation of T403 to the air surface leaves the near-surface region even further depleted of T403. This leads to a highly imperfect network and a high degree of swelling over a relatively large length scale. With the 46 phr sample, preferential segregation of T403 also leads to a depletion of T403 in the near-surface region; however, the composition will be much closer to the stoichiometric ratio, and thus the network is not nearly as imperfect as for the 36 phr sample. With the 56 phr sample, T403 would be in excess if resin and cross-linker were uniformly
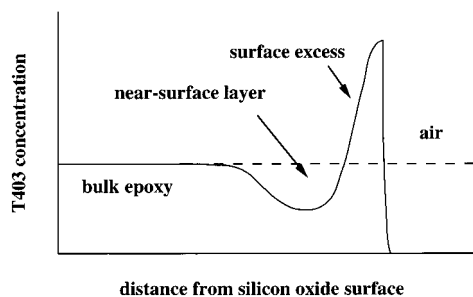
Figure 4. Qualitative illustration of the composition perturbation near the air surface. Strong segregation of the cross-linker to the air surface likely leads to a deletion of cross-linker in the near-surface region.

distributed. Depending upon the degree of preferential segregation of T403, the composition in the near-surface layer may actually approach the stoichiometric ratio. Thus, the surface region swells the least in this case, due primarily to the excess T403 immediately at the surface.

As shown in Figure 3b, a thin region of low SLD is detected near the silicon oxide surface for the 36 and 56 phr films. The length scale of this region is roughly 10 Å, much smaller than that of the layer of excess d-NB at the air surface. This indicates exclusion of d-NB from the region immediately adjacent to the substrate surface, apparently due to strong binding between epoxy and the native silicon oxide. The effect on the NR data is weaker than that of the excess d-NB layer at the air surface but is still very significant for the 36 phr sample. The effect of the depletion layer on the reflectivity is more subtle for the 56 phr sample. The reflectivity for the 46 phr film is insensitive to the presence or absence of a depletion layer of this magnitude, so a determination cannot be made in that case.

Finally, we note that the amount of d-NB in the bulk of the film is much higher for the 36 phr sample than for the other two compositions, indicating a lower cross-link density for the 36 phr composition. We also note that the roughness of the air surface for the 56 phr sample after swelling is much greater than that of the other samples.[49] We will return to this point later in the discussion.

Figure 5a compares NR data from 36, 46, and 56 phr films with cure B after swelling to equilibrium with d-NB. The best-fit SLD profiles are shown in Figure 5b. With the elevated temperature cure, it is expected that cross-linking occurs before the equilibrium composition profiles at the interfaces are approached. Indeed, the reflectivity curves in Figure 5a show two distinct differences from those of the films cured at room temperature. First, the reflectivity over the q range 0.01 Å^{-1} < q < 0.04 Å^{-1} for the 36 phr sample is comparable to that for the other samples. The very high reflectivity observed over this q range for the 36 phr sample with cure A is not observed with cure B. Thus, preferential segregation of T403 occurs to a much lesser extent with cure B. This is likely due to a competition between the rates of reaction and segregation. The degree of excess d-NB in the near-surface region for the three compositions with cure B occurs in the following order: 36 phr ≥ 46 phr > 56 phr. Second, for the 46 phr film the Kiessig fringes are much stronger with cure B than with cure A. The magnitude of the Kiessig fringes is determined by the SLD of the film relative to that of the substrate and air. Strong fringes result if the SLD is
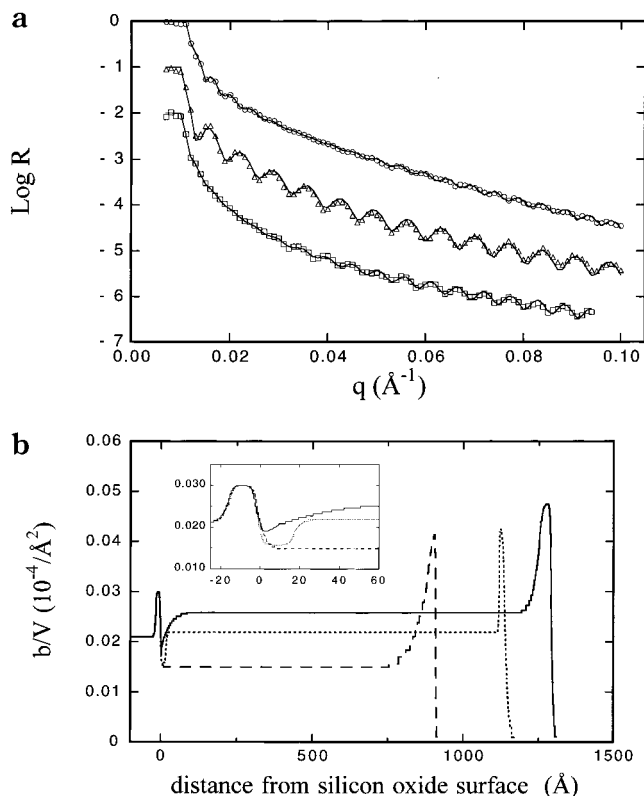

Figure 5. (a) Neutron reflectivity data from 36 (○), 46 (△), and 56 phr (□) samples (cure B) after swelling to equilibrium with d-NB. The data have been shifted on the y-axis for clarity. The curves through the data correspond to best fits using model scattering length density profiles. (b) Best-fit scattering length density profiles corresponding to the curves through the data in (a) for 36 (—), 46 (- - -), and 56 phr (· · ·) samples. The inset shows the depletion layer of d-NB at the substrate surface.

intermediate between that of silicon and air or is substantially greater than that of silicon. In the case of the 46 phr film with cure B, strong fringes result because the SLD is intermediate between that of silicon and air, as shown in Figure 5b. The Keissig fringes are weak for cure A because the SLD is comparable to that of silicon. Thus, cure B results in a much lower equilibrium concentration of d-NB within the 46 phr film than cure A, indicating that with cure B the network is more highly cross-linked or has fewer defects.

We note that again a significant depletion of d-NB is observed at the substrate surface for the 36 and 56 phr samples with cure B. The magnitude of this effect is substantially greater for cure B than for cure A. The reason for this is not clear. Such a layer is not required by the data for the 46 phr sample with cure B, as the data for this composition are again insensitive to this effect.

The degree of swelling within the bulk of the films is examined in Figure 6. This plot shows the volume fraction of d-NB as a function of T403 concentration for the equilibrated samples, where only the SLD of the central portion of the film was used in the calculation. Interestingly, there is a large variation in the degree of swelling with cure temperature for the 46 phr epoxy films, whereas only a very small variation with cure temperature is observed for the 36 and 56 phr films. The lower volume fraction d-NB for the 46 phr sample with cure B indicates a network that has achieved a higher cross-link density than is obtained with cure A.
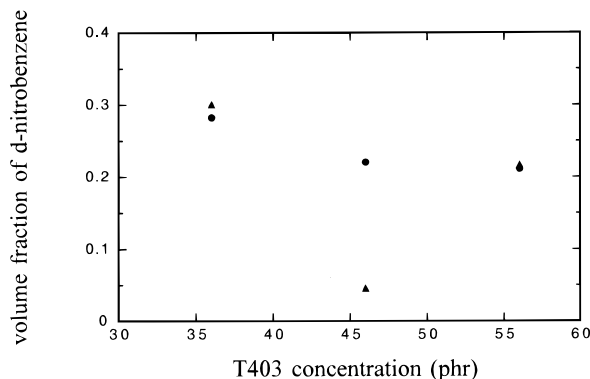
Figure 6. Volume fraction of d-NB as a function of T403 concentration for cure A (●) and cure B (▲). Note that the volume fraction is determined only from the scattering length density of the central portion of the film and does not include the interfacial regions.

The most likely explanation is that the epoxide–amine reaction does not go to completion in 48 h at 50 °C for the 46 phr composition but does go to completion for the 36 and 56 phr samples. The available kinetic data indicate only that the reaction goes to completion in roughly 24 h at 50 °C for 36 phr.[47] Indeed, DMA measurements suggest that bulk samples of nearly stoichiometric composition are not fully cured following cure A.[50] The fact that the central portions of the 36 and 56 phr films are not strongly affected by cure temperature argues against an explanation based on the competition between the rates of reaction and segregation. Further experiments on the extent of cure are underway to resolve this.

As shown in Figure 6, the swelling ratios of the epoxy films with off-stoichiometric compositions are not symmetric, regardless of curing conditions. Rather, a higher swelling ratio results for the 36 phr film than for the 56 phr film for both curing conditions. This is consistent with the results of bulk swelling experiments for the same epoxy/cross-linker system reported by Morgan et al.[30] They concluded that a more rapid increase in the molecular weight between cross-links (M_c) with deviation from the stoichimetric composition occurs on the excess epoxide side than on the excess T403 side. A similar conclusion has been reported by others.[51,52] This can be understood by considering the functionality of the resin and cross-linker and the network structures. As the fraction of T403 decreases below the stoichiometric ratio, unreacted epoxide groups are present and form dangling chain ends. The size and number of defects in the network become larger as the number of unreacted epoxide groups increases. As the amount of T403 decreases to 23.7 phr, M_c increases to infinity.[30] On the T403-rich side, all epoxide groups are reacted completely and unreacted amine groups are present. However, the effect of unreacted amine groups on the network structure is not as dramatic because each amine group has two reactive protons. If it is assumed that all primary amines react with epoxide groups prior to the onset of secondary amine–epoxide reactions, ring and branched network structures form even up to 94.7 phr.[30]

Figure 7 shows film thicknesses for the as-prepared and d-NB-swelled samples as a function of T403 concentration. The thickness is determined from the spacing of the fringes in the reflectivity curves and is thus determined independently of the d-NB volume fraction.
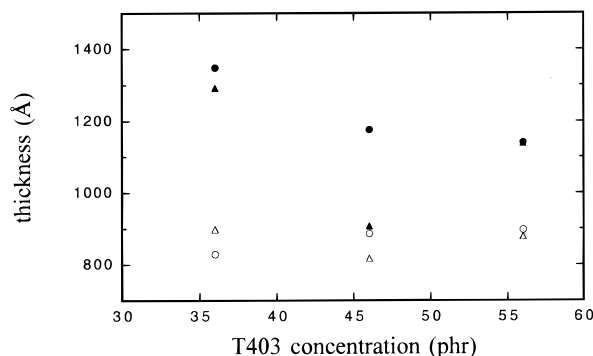
Figure 7. Film thickness as a function of T403 concentration for samples as-prepared (○) and after swelling (●) with cure A and as-prepared (△) and after swelling (▲) with cure B.
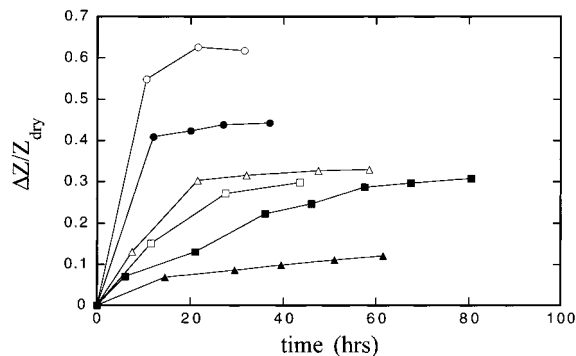

Figure 8. Relative change in film thickness ($\Delta Z/Z_{dry}$) vs time (t) for 36 (○), 46 (△), and 56 phr (□) samples with cure A and for 36 (●), 46 (▲), and 56 phr (■) samples with cure B.

The trends are consistent with the volume fraction data shown in Figure 6. The 46 phr film with cure B shows a much smaller increase in film thickness upon swelling compared to that with cure A. The 36 and 56 phr film thicknesses show a large increase upon swelling for both cure conditions. The swelled thickness of the 56 phr films are nearly independent of cure temperature, whereas for the 36 phr films a greater increase in thickness with swelling occurs with cure A than with cure B. The difference for the 36 phr film is due to the much greater excess swelling in the near-surface region for cure A. Such a trend does not appear in Figure 6 because only the central portion of each film was used in the d-NB volume fraction calculations.

Kinetics of Swelling. Since the equilibration time (>24 h) was much greater than the measurement time (4 h), certain aspects of the kinetics could be examined by monitoring the reflectivity as a function of time. The phenomena governing these rather long time processes are not clear. Diffusion of d-NB through the films is not the controlling process, as diffusion of a good solvent through the ultrathin films takes place on a time scale that is short compared to the measurement time. Indeed, no gradients in d-NB through the bulk of the films were detected even at the shortest exposure times examined (~6 h). The reflectivity data would be quite sensitive to such an effect if it were present. Apparently, the time for solvent to equilibrate within the film is short compared to the time for plasticizing or softening of the network. Thus, this study probes the relaxation of the network when subjected to a swelling pressure, rather than the rate of adsorption and diffusion of d-NB.

Figure 8 shows the relative change in film thickness ($\Delta Z/Z_{dry}$) vs time (t) for each sample. Several general
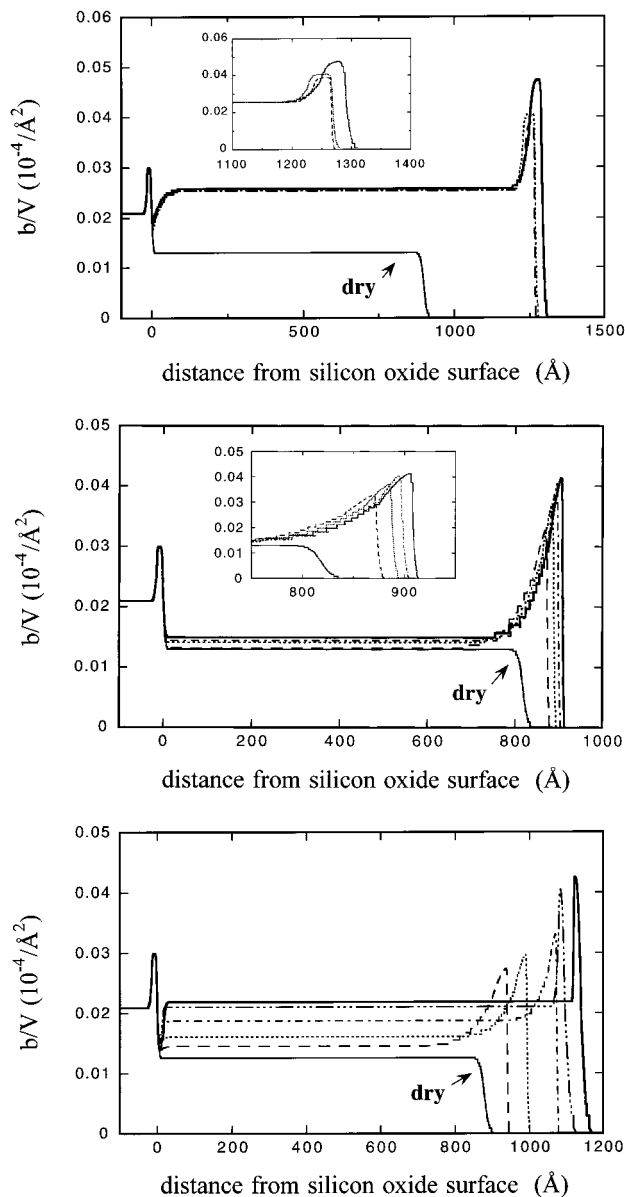
Figure 9. Scattering length density profiles for (a) 36 phr sample as-prepared (thin —) and after exposure to d-NB for 12 h (- - -), 20 h (· · ·), and 27 h (bold —); (b) 46 phr sample as-prepared (thin —) and after exposure to d-NB for 14.5 h (- - -), 29.5 h (· · ·), 39.5 h (-··-), and 51 h (bold —); (c) 56 phr sample as-prepared (thin —) and after exposure to d-NB for 6 h (- - -·), 21 h (· · ·), 36 h (-··-), 46 h (-···), and 67.5 h (bold —) with cure B. The insets for (a) and (b) show enlargements of the near-surface region.

trends are observed. First, the initial rates of swelling for 36 phr films are much greater than those for the 46 and 56 phr films. This can be understood in terms of the more imperfect network structures of T403-deficient compositions relative to resin-deficient compositions discussed earlier. Second, the initial rate of swelling is much greater for the 46 phr film cured at low temperature than for the 46 phr film cured at elevated temperature. (Low time data for 36 and 56 phr are insufficient to draw conclusions.) This can again be explained by a more rapid relaxation under swelling pressure for a more imperfect network structure.

Figure 9a–c shows SLD profiles as a function of time exposed to saturated d-NB for the 36, 46, and 56 phr films, respectively, with cure B. As shown in Figure 9a, the 36 phr film shows a large increase in film thickness

at relatively short exposure times (12 h) due to swelling of the bulk of the film. Data at sufficiently short times were not obtained to resolve the initial penetration of d-NB into the film. As time proceeds, only a small increase in film thickness occurs, mainly due to increased swelling near the air surface. The 46 and 56 phr films in Figures 9b and 9c show a distinctly different swelling behavior than the 36 phr film. For the 46 and 56 phr films, swelling is initially detected in the near-surface region, followed by gradual swelling of the center of the film. For the 46 phr film, the roughness of the air surface decreases from 3.5 to 1.7 Å upon initial swelling. The magnitude of the swelling at the air surface then continues to increase with time while the roughness at the air surface remains low. The 56 phr film shows a similar swelling behavior as for the 46 phr film during an initial period. However, between 36 and 46 h, the roughness at the air surface of the 56 phr film suddenly becomes greater, and the interface between the near-surface layer and the center of the film becomes sharper. We suggest that swelling stresses cause scission of some network strands at weak points for the 56 phr films, leading to roughening at the air surface. Nevertheless, an apparent steady state appears to be approached at long times (68 h). The very clear difference in swelling behavior between the 36 and 56 phr films revealed in Figure 9 is again attributed to the more imperfect network structures of T403-deficient compositions relative to resin-deficient compositions.

Conclusions

NR from epoxy films swelled with d-NB reveals variations in SLD at both the air surface and the silicon substrate surface. Excess swelling of d-NB at the air surface is observed for all the films. This indicates a lower cross-link density and is due to preferential segregation of the cross-linker to the air surface. The degree of excess swelling at the air surface depends on both the bulk epoxy composition and the cure temperature. To our knowledge, this effect has not been previously reported and may have important implications for multilayer paint films and other applications where thermosetting films are deposited and cured sequentially. A thin (~10–20 Å) layer depleted of d-NB at the substrate surface is also required to fit the NR data for the 36 and 56 phr films. For the 46 phr film, the sensitivity to this feature is very low, such that a clear determination about the presence of this layer cannot be made. The depletion of d-NB may be due to strong binding between the epoxy and the substrate. The effect is greater for films cured at elevated temperature than for films cured at room temperature. Large length-scale variations in cross-link density, such as have been reported at interfaces of epoxy with aluminum[31−33] and germanium,[36] were not observed at the silicon oxide surface. Asymmetry in the network structure with departure from stoichiometric composition is observed from the equilibrium degree of swelling, as well as from the relative rates. This is consistent with previous reports for bulk samples.

References and Notes

(1) Muller-Buschbaum, P.; Gutmann, J. S.; Lorenz, C.; Schmitt, T.; Stamm, M. *Macromolecules* **1998**, *31*, 9265.
(2) Zheng, X.; Rafailovich, M. H.; Sokolov, J.; Strzhemechny, Y.; Schwarz, S. A.; Sauer, B. B.; Rubinstein, M. *Phys. Rev. Lett.* **1997**, *79*, 241.
(3) Frank, B.; Gast, A. P.; Russel, T. P.; Brown, H. R.; Hawker, C. *Macromolecules* **1996**, *29*, 6531.
(4) Lee, Y. C.; Bretz, K. C.; Wise, F. W.; Sachse, W. *Appl. Phys. Lett.* **1996**, *69*, 1692.
(5) Wallace, J. W. E.; van Zanten, H.; Wu, W. L. *Phys. Rev. Lett.* **1995**, *52*, 3329.
(6) Hall, D. B.; Torkelson, J. M. *Macromolecules* **1998**, *31*, 8817.
(7) Frank, C. W.; Rao, V.; Despotopoulou, M. M.; Pease, R. F. W.; Hinsberg, W. D.; Miller, R. D.; Rabolt, J. F. *Science* **1996**, *273*, 912.
(8) Sutandar, P.; Ahn, D. J.; Franses, E. I. *Macromolecules* **1994**, *27*, 7316.
(9) Doruker, P.; Mattice, W. L. *Macromolecules* **1999**, *32*, 194.
(10) Rouse, J. H.; Twaddle, P. L.; Ferguson, G. S. *Macromolecules* **1999**, *32*, 1665.
(11) Forest, J. A.; Dalnoki-Veress, K.; Stevens, J. R.; Dutcher, J. R. *Phys. Rev. Lett.* **1996**, *77*, 2002.
(12) Tanaka, K.; Taura, A.; Ge, S.; Takahara, A.; Kaijiyama, T. *Macromolecules* **1996**, *29*, 3040.
(13) Reiter, G. *Europhys. Lett.* **1993**, *23*, 579.
(14) Hester, J. F.; Banerjee, P.; Mayes, A. M. *Macromolecules* **1999**, *32*, 1643.
(15) Hopkinson, I.; Kiff, F. T.; Richards, R. W.; Affrossman, S.; Hartshorne, M.; Pethrick, R. A.; Munro, H.; Webster, J. R. P. *Macromolecules* **1995**, *28*, 627.
(16) Hariharan, A.; Kumar, S. K.; Russell, T. P. *J. Chem. Phys.* **1993**, *98*, 4163.
(17) Schwarz, S. A.; Wilkens, B. J.; Pudensi, M. A. A.; Rafailovich, M. H.; Sokolov, J.; Zhao, X.; Zheng, X.; Russell, T. P.; Jones, R. A. L. *Mol. Phys.* **1992**, *76*, 937.
(18) Affrossman, S.; Bertrand, P.; Hartshorne, M.; Kiff, T.; Leonard, D.; Pethrick, R. A.; Richards, R. W. *Macromolecules* **1996**, *29*, 5432.
(19) Schaub, T. F.; Kellogg, G. J.; Mayes, A. M.; Kulasekere, R.; Ankner, J. F.; Kaiser, H. *Macromolecules* **1996**, *29*, 3982.
(20) Jalbert, C. J.; Koberstein, J. T.; Balaji, R. *Macromolecules* **1994**, *27*, 2409.
(21) Elman, J. F.; Koberstein, J. T.; Long, T. E. *Macromolecules* **1994**, *27*, 5341.
(22) Mansfield, K. F.; Theodorou, D. N. *Macromolecules* **1991**, *24*, 6283.
(23) Bitsanis, I.; Hadziioannou, G. J. *J. Chem. Phys.* **1990**, *92*, 3827.
(24) Yethiraj, A.; Hall, C. K. *Macromolecules* **1990**, *23*, 1865.
(25) de Gennees, P. G. *C. R. Acad. Sci., Ser. II* **1988**, *307*, 1841.
(26) Kumar, S. K.; Vacatello, M.; Yoon, D. Y. *J. Chem. Phys.* **1988**, *89*, 5206.
(27) Russell, T. P.; Lambooy, P.; Barker, J. G.; Gallagher, P.; Satija, S. K.; Kellogg, G. J.; Mayes, A. M. *Macromolecules* **1995**, *28*, 787.
(28) Wu, W.; Orts, W. J.; van Zanten, J. H.; Fanconi, B. M. *J. Polym. Sci.* **1994**, *32*, 2475.
(29) Fernandez, M. L.; Higgins, J. S.; Penfold, J.; Shackleton, C. S. *Polym. Commun.* **1990**, *31*, 124.
(30) Morgan, R. J.; Kong, F.; Walkup, C. M. *Polymer* **1984**, *25*, 375.
(31) Arayasantiparb, D.; Siangchaew, K.; Libera, M.; McKnight, S. Manuscript in preparation.
(32) Arayasantiparb, D.; Siangchaew, K.; Libera, M.; McKnight, S. *Microsc. Microanal.* **1997**, *3* (Suppl. 2), 543.
(33) Libera, M.; Zukas, W.; Wentworth, S.; Patel, A. In *Polymer/Inorganic Interfaces*; Drzal, L. T., Opila, R. L., Peppas, N., Schutte, C., Eds.; *MRS Symp. Proc.* **1995**, *385*, 65.
(34) Dillingham, R. G.; Boerio, F. J. *J. Adhes.* **1987**, *24*, 315.
(35) Buchwalter, L. P.; Greenblatt, J. *J. Adhes.* **1986**, *19*, 257.
(36) Garton, A. *J. Polym. Sci., Polym. Chem. Ed.* **1984**, *22*, 1495.
(37) Chan, C. M. *J. Adhes.* **1983**, *15*, 217.
(38) Comyn, J.; Horley, C. C.; Oxley, D. P.; Pritchard, R. G.; Tegy, J. L. *J. Adhes.* **1981**, *12*, 171.
(39) Racich, J. L.; Koutsky, J. A. In *Chemistry and Properties of Crosslinked Polymers*; Labana, S. S., et al., Eds.; Academic Press: New York, 1977; p 303.
(40) Flory, P. J. *Principles of Polymer Chemistry*; Cornell University Press: Ithaca, NY, 1983.
(41) Horkay, F.; Hecht, A. M.; Geissler, E. *Macromolecules* **1998**, *31*, 8851.
(42) Falcão, A. N.; Pedersen, J. S.; Mortensen, K. *Macromolecules* **1993**, *26*, 5350.
(43) Soni, V. K.; Stein, R. S. *Macromolecules* **1990**, *23*, 5257.
(44) Wu, W. L.; Hunston, D. L. K.; Yang, H.; Stein, R. S. *Macromolecules* **1988**, *21*, 756.
(45) Davidson, N. S.; Richards, R. W.; Maconnachie, A. *Macromolecules* **1986**, *19*, 431.
(46) Certain trade names and company products are identified in order to specify adequately the experimental procedure. In no case does such identification imply recommendation or endorsement by the National Institute of Standards and Technology, nor does it imply that the products are necessarily the best for the purpose.
(47) Chiao, T. T.; Moore, R. L. *Proceedings of the 29th Conference of Reinforced Plastics/Composites Division of SPI*, Washington, D.C.; Section 16-B, 1, 1974.
(48) Russell, T. P. *Mater. Sci. Rep.* **1990**, *5*, 171.
(49) The roughness of the air surface is indicated in the SLD plots by an increased interfacial width. However, the roughness is more likely an in-plane effect which cannot be represented in the depth profile plots.
(50) Reedy, E. D. Sandia National Laboratories, unpublished data. These measurements involved slightly different conditions than the work reported here. Samples with 43 phr T403 were cured at 50 °C for 24 h and then 40 °C for 24 h. The glass transition temperature by DMA was initially measured to be roughly ~60 °C. The sample was then heated to 80 °C and held for several hours. After cooling to room temperature, the glass transition temperature was measured again and had increased to 75−80 °C.
(51) Meyer, F.; Sanz, G.; Mondragon, I.; Mijovic, J. *Polymer* **1995**, *36*, 1407.
(52) Ferandez-Nograro, F.; Valea, A.; Llano-Ponte, R.; Mondragon, I. *Eur. Polym. J.* **1996**, *32*, 257.

MA990990C